JOURNAL OF NATURAL PRODUCTS

pubs.acs.org/jnp

Article

Anthracaurisin A—Discovery of a Cytotoxic *Nor*-Sesquiterpene Dimer from Patagonian *Anthracophyllum discolor*

Bastien Petit, Ines Michrafy, Jordan Nafie, Grayce E. Dyer, Erin M. Marshall, Cristian Riquelme, Jaime R. Cabrera-Pardo, James A. Strother, and Sandra Loesgen*

Cite This: *J. Nat. Prod.* 2026, 89, 1995−2007

Read Online

ACCESS | Metrics & More | Article Recommendations | Supporting Information

ABSTRACT: Fungal natural products, also called secondary metabolites (SMs), continue to inspire chemists and drug development. Around 30,000 fungal SMs are known, mainly from filamentous fungi of the phylum Ascomycota. Only 5% of all fungal species are described today, and even fewer have been cultured or chemically screened, which makes fungi an untapped reservoir for chemical discovery. The phylum Basidiomycota harbors chemically talented fungi such as the psilocybin producer *Psilocybe cubensis* (Agaricales, Hymenogastraceae), but other members like the genus *Anthracophyllum* (Agaricales, Omphalotaceae) remain largely genetically and chemically underexplored although new species are being discovered frequently. Here, we present the chemical and bioactivity exploration of a Chilean *Anthracophyllum discolor* fungus. We discovered anthracaurisin A, the first fungal *nor*-sesquiterpene homodimer with potent cytotoxic activity *in vitro* and *in vivo*, isolated one new and several known illudins, and established their absolute configurations.

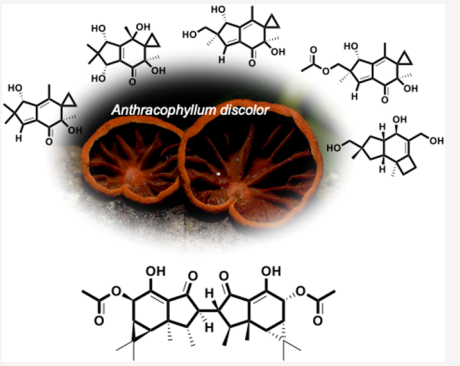

Fungi are prolific producers of natural products, also called secondary metabolites (SMs). An estimated 30,000 fungal SMs are known, mainly from filamentous fungi of the phylum Ascomycota.[1] Estimates indicate that only 5% of all extant fungal species have been described, and even fewer have been cultured or chemically screened, suggesting that fungi remain an untapped reservoir for SMs discovery.[2] From Ascomycota alone, which includes well-studied genera such as *Aspergillus*, *Fusarium*, and *Penicillium*, a conservatively estimated 1.4 million compounds remain to be discovered.[1] The chemical diversity of fungal metabolites and their potential for human health applications can be seen in clinically used drugs from Ascomycota such as the immunosuppressing agent cyclosporin from *Tolypocladium inflatum*, the cholesterol-lowering lovastatin from *Aspergillus terreus*, and the antibiotic penicillin from *Penicillium rubens*. In recent years, more SMs from the phylum Basidiomycota have been discovered,[3] and there has been reinvigorated interest in psilocybin from *Psilocybe cubensis* for its biosynthesis and to develop and treat neurological disorders.[4]

The genus *Anthracophyllum* (Agaricales, Omphalotaceae) includes about 12 species of pleurotoid/marasmioid Basidiomycetes fungi growing in tropical regions of the world.[5] Our literature review revealed that new *Anthracophyllum* species are being continuously discovered, but no genome sequences are available for the family of Omphalotaceae, and only a few partial gene loci amplifications can be found for *Anthracophyllum lateritium*, *A. archeri*, *A. sinensis*, and *A. sontraense*.[6,7] In the past, morphological criteria placed this genus in the Marasmiaceae family, but modern taxonomic criteria place *Anthracophyllum* within the Omphalotaceae family.[8,9] Macroscopically, *Anthracophyllum* species are well-known for the pigmentation of their basidiomes, with colors from orange to reddish-brown but also black or dark blue depending on the species. A blue-green coloration is typically observed when treating the basidiomes with aqueous alkali due to the presence of various terphenyl derivatives including cycloleucomelon.[10,11] Another natural product study has reported the occurrence of sesquiterpenoids including the class of aristolane sesquiterpene dimers called aurisins.[8] Aside from this, very little is known regarding the SMs synthesized by *Anthracophyllum*, which has been studied for its ability to degrade organic matter and its bioremediation potential.[12−15]

In an ongoing effort to discover new and bioactive natural products, we screened a set of Chilean−Patagonian basidiomycetes for antimicrobial, cytotoxic, and pain-relieving activities.[16,17] The screening identified an *Anthracophyllum discolor* extract (internal strain name JCP1718), grown on rice-based media, with potent antibacterial and cytotoxic activities. Mass spectrometry (MS)-based dereplication efforts supported the presence of potentially unique chemical features.

Here, we report the isolation and bioactivity of six terpenoids related to the illudane class of natural products. The known

Received: April 24, 2026
Revised: May 29, 2026
Accepted: June 2, 2026
Published: June 11, 2026

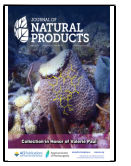

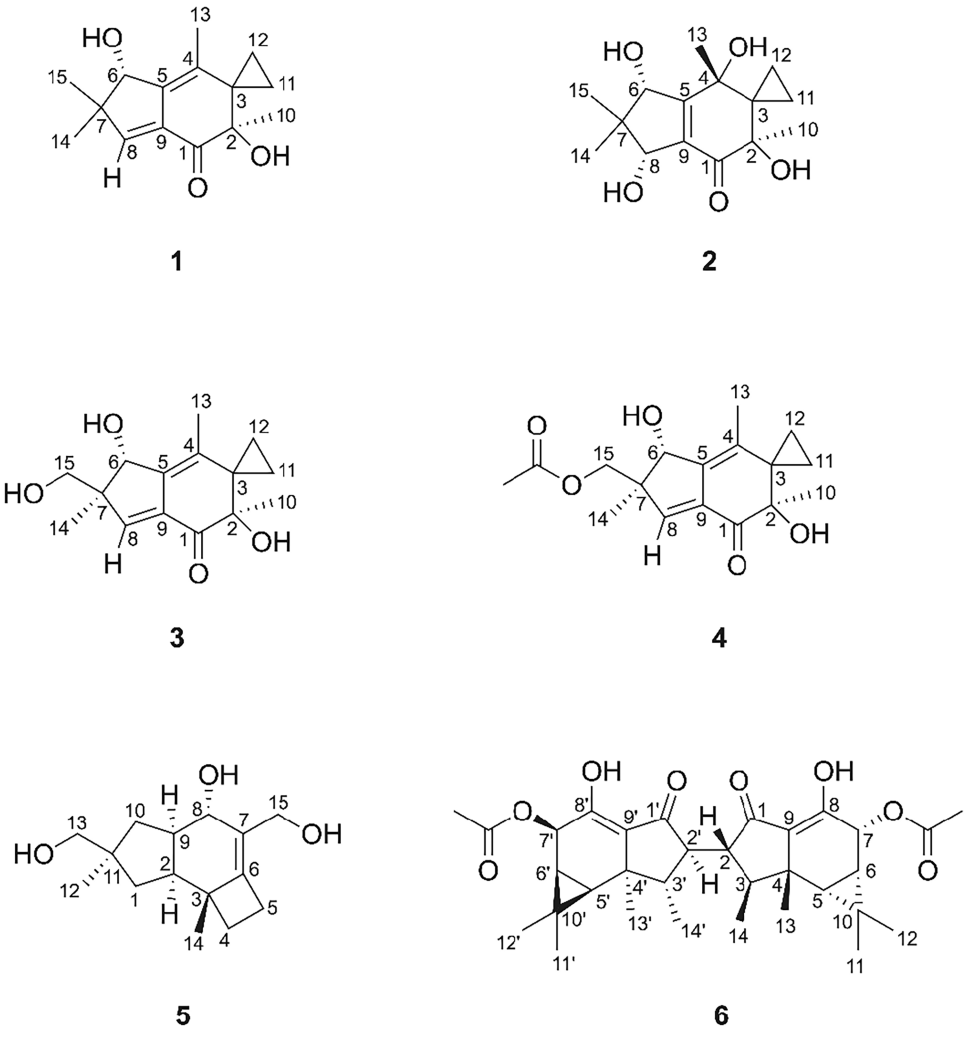

Figure 1. Structures of compounds **1** to **6**. Compounds **4** and **6** are previously undescribed.

illudanes (**1**, **2**, **3**, and **5**) were subjected to stereochemical analysis using ECD and VCD spectroscopy supported by DFT-based computations to unequivocably assign their absolute configuration for the first time. We also found one new illudane (**4**) as well as a unique *nor*-sesquiterpene dimer scaffold with potent cytotoxicity, which we named anthracaurisin A (**6**).

RESULTS AND DISCUSSION

A set of Patagonian Basidiomycetes was collected in Chile and identified based on macroscopic and microscopic observations, which was supported by ITS sequencing. These fungi were grown in two media conditions (solid rice and liquid malt), each extracted using two different solvents (ethyl acetate and methanol). The resulting extracts were screened in multiple bioassays: (i) for antimicrobial activity against human pathogens (including *Staphylococcus aureus*, multidrug-resistant *S. aureus*, *Escherichia coli*, and *Candida albicans*), (ii) for inhibition of cell viability using a human colon cancer cell line (HCT-116), and (iii) for *in vivo* effects in a zebrafish acute toxicity assay.[17] One extract, *A. discolor* grown on rice and extracted with ethyl acetate, exhibited potent antistaphylococcal activity and toxic activity *in vitro* and *in vivo*. In parallel, all extracts were subjected to a chemical dereplication approach using high-resolution LC-MS and LC-MS/MS with the aim of avoiding the isolation of known fungal metabolites. The bioactive *A. discolor* extract exhibited unique MS features with m/z values of 435.2559 (ESI +) and 553.2831 (ESI −), which could not be matched with known metabolites from our in-house UV database and online/commercial databases.[18,19] Moreover, the mass spectrometric feature was considerably more abundant in the solid rice extracts than the liquid malt extracts, suggesting its occurrence to be highly dependent on the growth medium conditions.

Structure Elucidation of Compounds 1 to 6

Six compounds were isolated from the ethyl acetate rice extract of *A. discolor*, including the known illudins M (**1**), B (**2**), S (**3**), and dichomitin A (**5**), together with the new 15-*O*-acetylilludin S (**4**) and anthracaurisin A (**6**). Their structures (Figure 1) were elucidated via extensive NMR and HRESIMS experiments. Stereochemical assignments were achieved using NOE NMR and ECD/VCD spectroscopic experiments, supported by DFT-based computations. Multiple stereoisomers of illudins **1**−**3** were previously isolated, however, with limited spectral data, and the absolute configuration of dichomitin A (**5**) was subjected to revision in the past. To unequivocally assign the absolute configuration of **1**, **2**, **3**, and **5**, we carried out a series of VCD and ECD experiments in conjunction with measuring their optical rotation.

Compound **1** was identified as illudin M based on mass spectrometry and NMR data (details in SI S49). However, its specific rotation (−44°) was significantly different from the

https://doi.org/10.1021/acs.jnatprod.6c00531
J. Nat. Prod. 2026, 89, 1995−2007

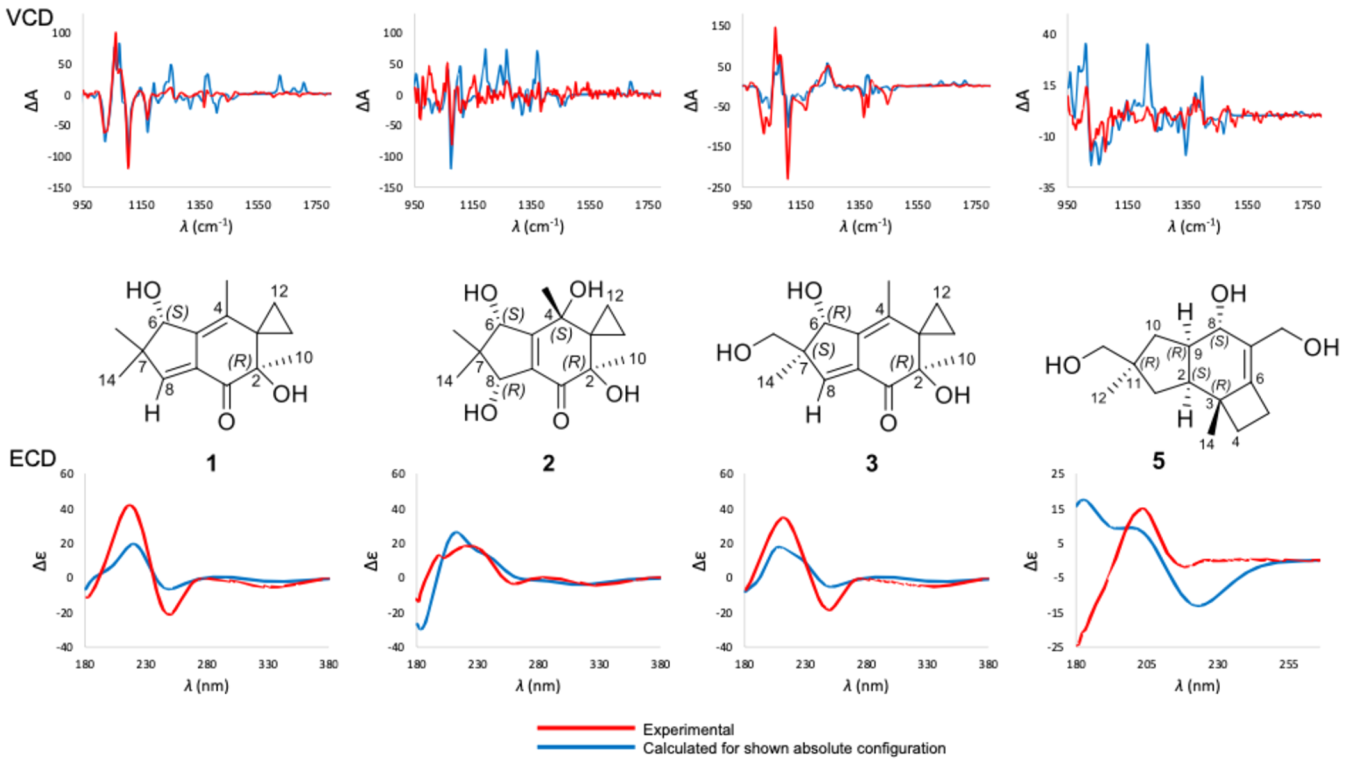

Figure 2. Experimental (red) and calculated (blue) VCD and ECD spectra of known compounds **1**, **2**, **3**, and **5**.

published specific rotation of illudin M ((2*R*,6*S*)-illudin M, −284°).[20,21] Multiple stereoisomers of illudin M have been described recently,[22] including (2*S*,6*R*)-illudin M with a reported specific rotation of +96° (named (3*S*,7*R*)-illudin M in the cited literature) and (2*S*,6*S*)-illudin M with a specific rotation of +59° (named (3*S*,7*S*)-illudin M in the cited literature). For further details on carbon numbering systems for illudins, please see Figure S66 in the SI. Despite similar experimental conditions, none of these specific rotation values matched ours (Table S52). We decided to use experimental and computational VCD and ECD approaches, which revealed compound **1** to be the original published illudin M ((2*R*,6*S*)-illudin M) by comparison to its DFT-calculated and experimental ECD/VCD data (Figure 2, details in SI S53−S55). Vibrational circular dichroism (VCD) is a powerful technique for the study of stereochemistry in the solution phase without derivatization.[23] Although ECD has been previously used for the stereochemical assignments of illudane sesquiterpenoids, to our knowledge, VCD is used here for the first time.[23−26] Multiple stereoisomers coexist in illudane literature, and the specific rotations alone are not sufficient to determine their stereochemistry. We believe our ECD/VCD-based approach toward the absolute configuration of illudins will be helpful to the community.

Compound **2** shared a number of similar NMR signals with compound **1** (details in SI S49). Its mass spectrometry data revealed its nominal mass to be 34 Da greater than that of compound **1**, which could suggest two additional hydroxy groups and a double bond reduction. Extensive 2D NMR analysis revealed the two supernumerary hydroxys to be located at C-4/C-8 and the reduction to involve the cross-conjugated dienone system spanning C-8, C-9, C-4, C-5, and C-1 of the illudin backbone. Two stereoisomers of this structure were previously described, known as illudin B and H.[27,28] ROESY NMR and specific rotation of compound **2** (−18°) shared many similarities with illudin B (−9°), but these resemblances were not considered sufficient for a stereochemical assignment given the 16 possible stereoisomers for this structure. Similarly to compound **1**, we performed VCD and ECD spectral analyses of compound **2** supported by DFT-based computations, which confirmed **2** to be illudin B ((2*R*,4*S*,6*S*,8*R*)-illudin B) (Figure 2, details in SI S56−S58).

Compound **3** was identified as illudin S based on mass spectrometry and NMR data (details in SI S49). Reminiscent of compound **1**, the specific rotation of compound **3** (−104°) was significantly different from the reported specific rotation of illudin S ((2*R*,6*R*,7*S*)-illudin S, − 358°)[20,21] and another stereoisomer of illudin S reported recently from the Basidiomycete *Granulobasidium vellereum*.[22] Again, experimental and computational VCD and ECD approaches were used to unambiguously assign compound **3** to have the 2*R*,6*R*,7*S* configuration of illudin S (Figure 2, details in SI S59−S61).

Compound **4**'s NMR data were almost superimposable to that of compound **3**, except for a key chemical shift difference at C-15 with δ_C 69.3/δ_H 3.39, 3.33 ppm for compound **3** and δ_C 70.6/δ_H 3.97, 3.93 ppm for compound **4** (Tables 1 and S49). 2D NMR experiments allowed the identification of an extra *O*-acetyl moiety located at C-15 in compound **4**, as demonstrated by the HMBC cross-peak of H_2-15 δ_H 3.97, 3.93 to δ_C 172.6 (15-*O*-Ac, C═O) (Figure 3). This was further supported by mass spectrometry evidence, in which compound **4** showed 42 additional mass units compared to compound **3**. The relative and absolute configuration of compound **4** seemed to be identical to compound **3** based on NMR chemical shifts, NOESY correlations, and specific rotations of similar sign and magnitude (compare Tables 1 with S49 for NMR, compare Figures 3 with S51 for NOESY correlations, and compare the new compounds description with Table S52 for specific

https://doi.org/10.1021/acs.jnatprod.6c00531
J. Nat. Prod. 2026, 89, 1995−2007

Table 1. ^{1}H and ^{13}C NMR Spectroscopic Data for Compound 4, 600 MHz, Methanol-d_4, Cryoprobe, 1.7 mm Tubes

	4	
position	δ_C, type	δ_H
1	201.4, C	
2	77.6, C	
3	32.8, C	
4	135.6, C	
5	139.4, C	
6	75.6, CH	4.59, s
7	54.1, C	
8	141.5, CH	6.39, s
9	137.1, C	
10	24.7, CH_3	1.36, s
11	8.9, CH_2	1.09, m; 0.44, m
12	6.2, CH_2	0.97, m; 0.79, m
13	14.3, CH_3	1.68, s
14	16.6, CH_3	1.18, s
15	70.6, CH_2	3.97, d (11.0); 3.93, d (11.0)
15-*O*-Ac (CO)	172.6, C	
15-*O*-Ac (Me)	20.5, CH_3	1.99, s

rotations). VCD and ECD experiments confirm this statement and assign the three stereocenters of **4** to be in the 2*R*,6*R*,7*S* configuration (Figure 4). Based on the above data, compound **4** was named 15-*O*-acetylilludin S. Although this compound has been previously synthesized as part of structure−activity studies on illudins, here is the first report of **4** as a natural product.[22,29,30]

Compound **5** NMR and mass spectrometry data were similar to the previously reported dichomitin A, also called dichomitol (Table S50).[31,32] Its chemical shifts and NOESY correlations were identical to dichomitin A, suggesting that both compounds shared the same relative and absolute configuration (Figure S51). However, the specific rotation of compound **5** (−5°) was of opposite sign of dichomitin A (+6.3°) (Table S52). VCD and ECD experiments assigned the absolute configuration of compound **5** to be 2*S*,3*R*,8*S*,9*R*,11*R*, identical to the dichomitin A structure published in 2004, however here with a different specific rotation value (Figure 2). This case illustrates nicely how stereochemical assignments based on NMR and specific rotation data can benefit from expanded spectral analyses and computations.

Compound **6** exhibited a molecular formula of $C_{32}H_{42}O_8$, deduced from its HRESIMS data showing a $[M-H]^-$ ion peak of m/z 553.2831 (calcd for $C_{32}H_{41}O_8^-$, 553.2807; mass error −4.34 ppm). An extensive analysis of its NMR data suggested **6** to be a dimer formed by the fusion of two illudane sesquiterpenoid monomers, which were not isolated nor detected from the fungus (Figure 1). Each monomer exhibited four methyls CH_3-11 (δ_C/δ_H 31.1/1.06), CH_3-12 (δ_C/δ_H 15.7/1.25), CH_3-13 (δ_C/δ_H 24.1/1.04), and CH_3-14 (δ_C/δ_H 12.3/1.06), one hydroxymethine CH-7 (δ_C/δ_H 66.9/5.92), one hydroxy-olefinic carbon C-8 (δ_C 164.4), one ketone C-1 (δ_C 204.4), one ester moiety (δ_C 171.1), and a *gem*-cyclopropyl unit at CH-5 (δ_C/δ_H 31.6/0.97) and CH-6 (δ_C/δ_H 26.5/1.32) (Table 2). The dimer is connected at C-2 based on the HMBC cross-peak between CH-2 and its dimeric equivalent CH-2′, at δ_C/δ_H 49.0/3.03 (Figure 3).

Compound **6**'s NMR data showed a phenomenon of duplication of some of the proton signals and most of the carbon signals with a consistent ratio of 1:0.6 between each signal and its duplicate equivalent, particularly apparent on the ^{13}C spectrum of **6** in $CDCl_3$ (Figure 5).

Variable temperature (VT) NMR experiments in DMSO-d_6 at 323, 348, and 373 K allowed coalescence of the previously duplicated ^{1}H and ^{13}C NMR signals at higher temperature, confirming that the two halves are identical, but that the compound exists as a pair of distinct *M* or *P* atropisomers (rotamers along the *C*-2/*C*-2′ axis) in solution, on the NMR time scale, at room temperature (Figure 5, Table S39). We named the (*P*) and (*M*) atropisomers accordingly, following the axial chirality nomenclature,[33,34] and assigned different chemical shifts to the atropisomers based on hydrogen bonding (Figure 6).

The relative and absolute configuration of **6** was established by VCD and ECD approaches supported by DFT calculations to be (2*R*,2′*R*,3*S*,3′*S*,4*S*,4′*S*,5*R*,5′*R*,6*S*,6′*S*,7*R*,7′*R*) (details S46−48).[35] Briefly, computed IR and VCD spectra at the B3PW91/cc-pVTZ DFT level were compared to their experimental counterparts both visually and via algorithmic (CompareVOA, BioTools, Jupiter, FL)[36] analysis (Figure 4, details Figures S46−S48). Quantitative comparisons of the experimental and DFT-derived IR and VCD spectra resulted in high similarity (S_{fg}) and enantiomeric similarity index values for the (2*R*,2′*R*,3*S*,3′*S*,4*S*,4′*S*,5*R*,5′*R*,6*S*,6′*S*,7*R*,7′*R*) configuration and a high confidence level (99%) assignment (Figure S48). To support the relative configuration, we calculated six alternate structures, varying the dimer connection stereochemistry, as well as inverting each stereocenter or pair of stereocenters in the cyclopropyl case, on both halves of the dimer, to see if any improvements to the spectral agreement were possible. In each case, the spectra were visibly a worse match and yielded lower similarity values. In addition, we obtained UV−vis and ECD

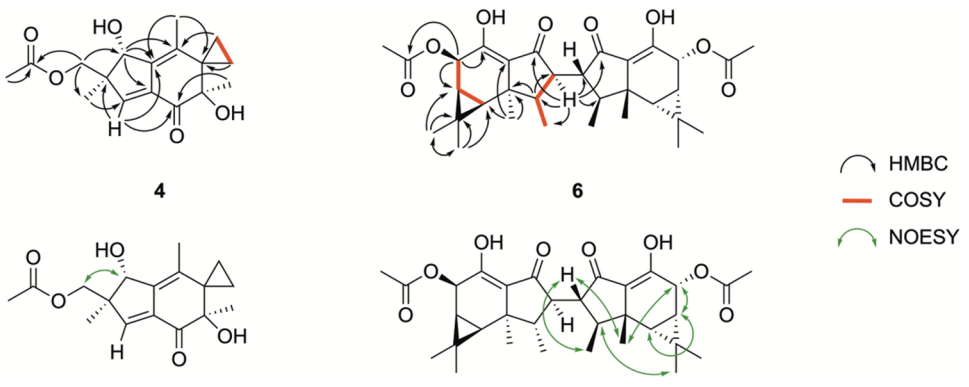

Figure 3. Key HMBC, COSY, and NOESY correlations of previously undescribed compounds **4** and **6**.

https://doi.org/10.1021/acs.jnatprod.6c00531
J. Nat. Prod. 2026, 89, 1995−2007

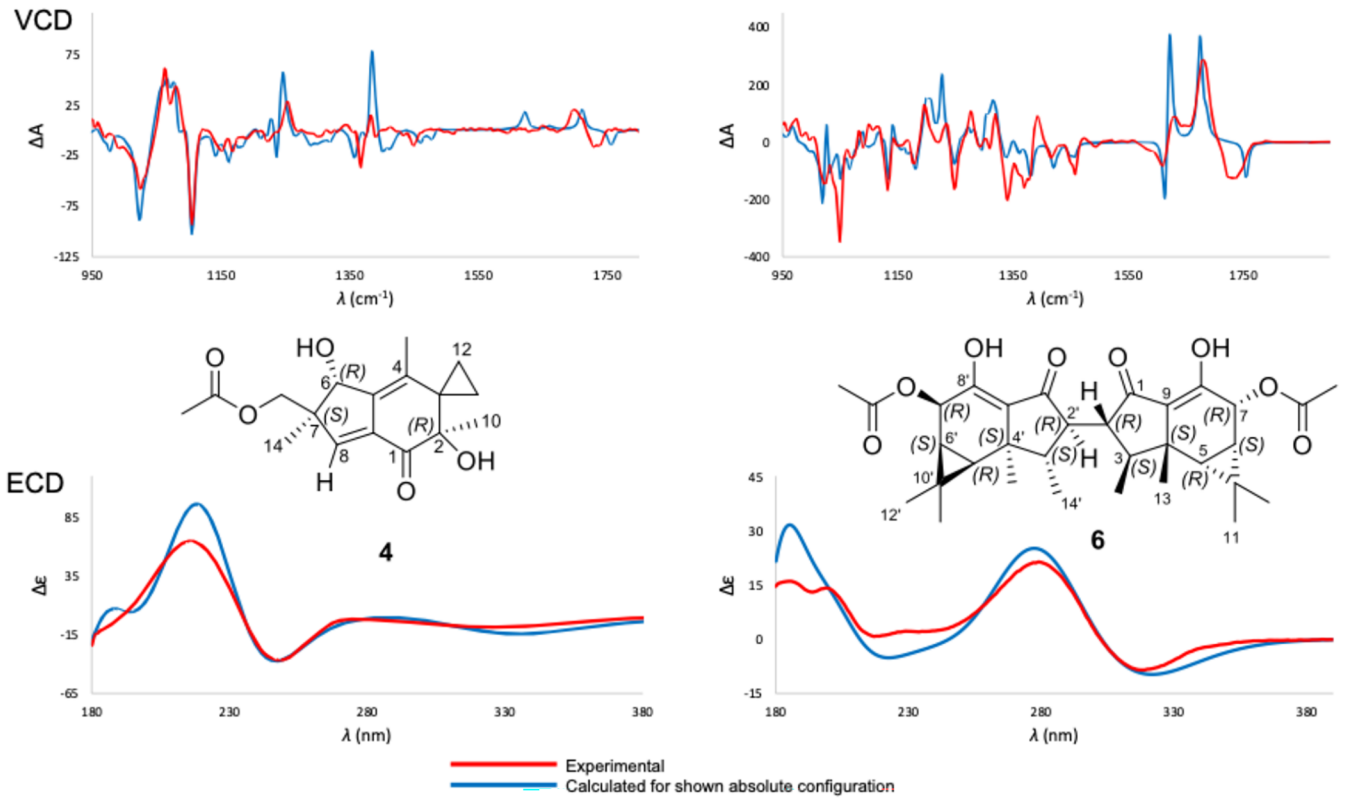

Figure 4. Experimental (red) and calculated (blue) VCD and ECD spectra of 15-*O*-acetylilludin S (**4**) and anthracaurisin A (**6**).

Table 2. ^{1}H and ^{13}C NMR Spectroscopic Data for (*P*) and (*M*) Atropisomers of 6, 500 MHz, Chloroform-*d*, *J* in Hz, ov., Overlapped

	P-**6**		*M*-**6**	
position	δ_C, type	δ_H	δ_C, type	δ_H
1/1′	204.4, C		205.5, C	
2/2′	50.0, CH	2.18, ov.	49.0, CH	3.03, br d (12.0)
3/3′	42.8, CH	2.65, m	40.6, CH	1.97, m
4/4′	41.0, C		41.2, C	
5/5′	31.6, CH	0.97, d (8.6)	31.4, CH	1.01, ov.
6/6′	26.5, CH	1.32, t (7.5)	26.7, CH	1.39, t (7.5)
7/7′	66.9, CH	5.92, br d (5.8)	66.5, CH	5.98, br d (5.8)
8/8′	164.4, C		163.5, C	
9/9′	117.2, C		116.6, C	
10/10′	21.4, C		21.4, C	
11/11′	31.1, CH_3	1.06, br s	30.9, CH_3	1.06, br s
12/12′	15.7, CH_3	1.25, br s	16.5, CH_3	1.14, br s
13/13′	24.1, CH_3	1.04, br s	24.3, CH_3	1.11, br s
14/14′	12.3, CH_3	1.06, ov.	13.3, CH_3	0.85, br d (6.1)
7/7′-*O*-Ac (CO)	171.1, C		170.9, C	
7/7′-*O*-Ac (Me)	21.0, CH_3	2.15, br s	21.0, CH_3	2.15, br s
8/8′-OH		6.80−7.60, bs s		6.80−7.60, br s

data for this compound, and the DFT-calculated spectra for the (2*R*,2′*R*,3*S*,3′*S*,4*S*,4′*S*,5*R*,5′*R*,6*S*,6′*S*,7*R*,7′*R*) configuration produced an excellent match to the experiment. Our stereochemical assignment is additionally supported by literature data: the aurisins are structurally related sesquiterpene dimers, produced by Basidiomycota genera *Panus*, *Neonothopanus*, and *Anthracophyllum*, and the aurisins share several stereocenters in the same configurations.[8,37,38] Compound **6** was thus named anthracaurisin A after the producing strain and the related class of aurisin terpenoids.[39] We were able to detect anthracaurisin A in rice cultures extracted with dichloromethane and acetonitrile, supporting the notion that this is a natural product and not an artifact of the ethyl acetate extraction.

Biosynthetic Hypothesis

Despite being related to the aurisins, **6** lacks a carbon per monomeric subunit (C_{14} monomer for anthracaurisin A instead of C_{15} monomer for the aurisins); therefore, it falls within the rare class of *nor*-sesquiterpene dimers. We propose that the biosynthesis starts with a sesquiterpene maaliane cation, a precursor for all aristolene monomers with the characteristic *gem*-dimethylpropane moiety also found in aurisins. Starting from the aristolene scaffold, we propose an early installment of the ketone and hydroxy groups, as seen in other members of this class of compounds (Figure 7).[40] Ring contraction from a six-membered cyclohexanone to a five-membered ring has been extensively studied in the gibberellin biosynthesis, which is catalyzed by a cytochrome P450 enzyme (CYP114) via a semipinacol rearrangement.[41] We propose a similar ring contraction, followed by oxidation of the excised aldehyde carbon and decarboxylation of the acid. The resulting radical species could undergo radical dimerization and give rise to **6**.[42,43]

Sesquiterpene dimers are rare in fungi, and the first report appears to be trichoderonic acid B, a dimer of the heptelidic acid sesquiterpene isolated from a Japanese *Trichoderma virens*.[44] More heptelidic acid dimer analogues were later characterized from the pleurotoid mushroom *Lentinellus ursinus* and a termite-associated *T. virens*.[45,46] Other examples are the disydonols A-C, phenolic bisabolane sesquiterpenoid dimers isolated from a marine *Aspergillus* species.[47] We next focused on *nor*-

https://doi.org/10.1021/acs.jnatprod.6c00531
J. Nat. Prod. 2026, 89, 1995−2007

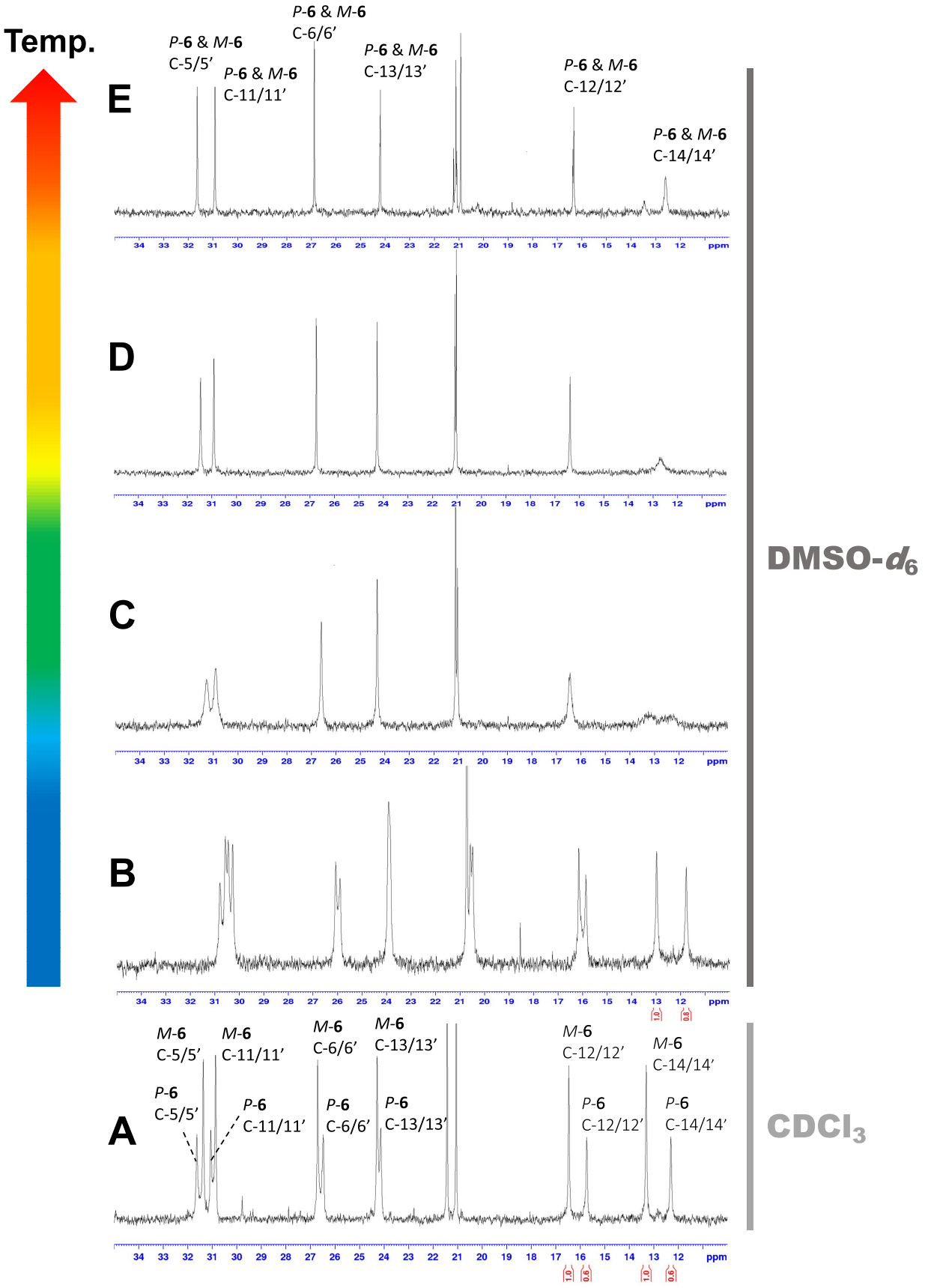

Figure 5. 10 to 35 ppm region of ^{13}C NMR spectrum of anthracaurisin A (**6**) exhibits doubled signals for C-5/5′, C-6/6′, C-11/11′, C-12/12′, C-13/13′, and C-14/14′ of the *P* and *M* atropisomers. (A) ^{13}C NMR spectrum of **6** in $CDCl_3$ at 298 K. (B) ^{13}C NMR spectrum of **6** in DMSO-d_6 at 298 K, (C) 323 K, (D) 348 K, and (E) 373 K.

https://doi.org/10.1021/acs.jnatprod.6c00531
J. Nat. Prod. 2026, 89, 1995−2007

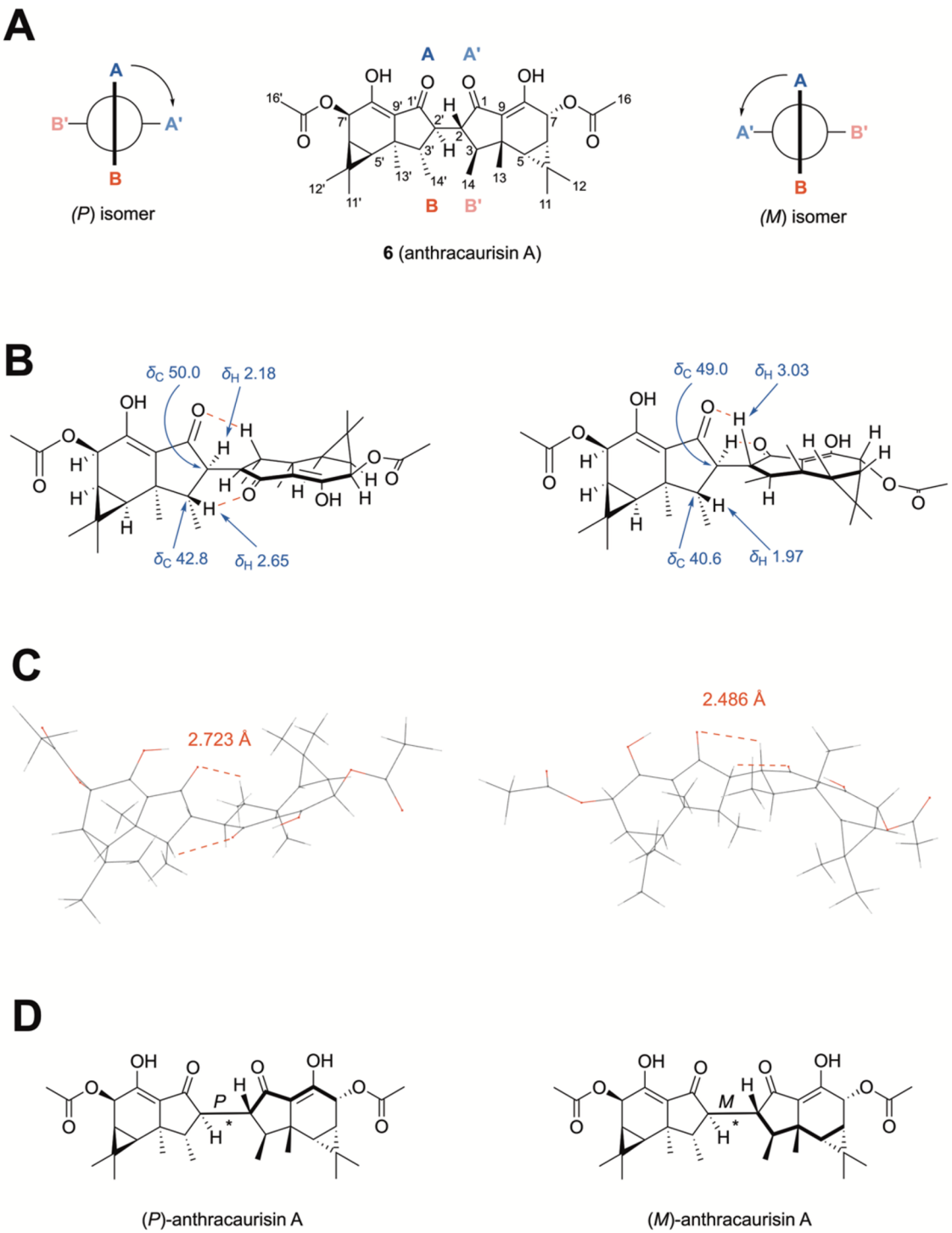

Figure 6. Structures of the *P* and *M* atropisomers of anthracaurisin A (**6**). (A) Definition of the *A*, *B*, *A*′, *B*′ axes of **6** and Newman projections of the two atropisomers, *P*-**6** (left) and *M*-**6** (right). (B) Perspective representation of *P*-**6** (left) and *M*-**6** (right) structures. ^{13}C and ^{1}H chemical shift differences for *P* and *M* conformers at C-2/C-2′ and C-3/C-3′ are emphasized in blue color and may be attributed to different, possible hydrogen bonding patterns (red dashed lines). (C) Wireframe representation of DFT-calculated lower-energy conformers of **6** generated in Avogadro software with hydrogen bonding in red dashed lines. (D) Flat representation of *P*-**6** (left) and *M*-**6** (right).

sesquiterpene homodimers from fungi (*i.e.*, sesquiterpene dimers composed of two *nor*-sesquiterpene subunits), and to the best of our knowledge, anthracaurisin A (**6**) is the first and only fungal example. Plants, however, are able to produce *nor*-sesquiterpene homodimers like mexicanin F isolated from *Helenium mexicanum* and valeriadimer A from *Valeriana officinalis*.[43,48] Plants are also known to synthesize *nor*-sesquiterpene heterodimers (*i.e.*, sesquiterpene dimers composed of one *nor*-sesquiterpene subunit and one sesquiterpene subunit) such as dinardokanshone A and valeriadimer B.[43,49] We believe anthracaurisin A is the first *nor*-sesquiterpene homodimer in fungi and one of the very few sesquiterpene dimer natural products.

https://doi.org/10.1021/acs.jnatprod.6c00531
J. Nat. Prod. 2026, 89, 1995−2007

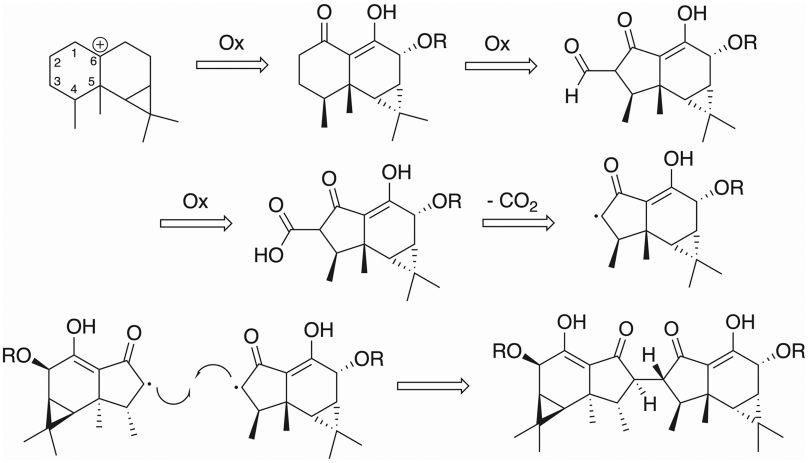

Figure 7. Putative biosynthetic pathway for anthracaurisin A (**6**).

Table 3. Antimicrobial Activity of Compound 6 against Various Human Pathogens (MIC90, μg/mL)[a,b,c]

pathogen	6	kanamycin[c]	vancomycin[c]	ampicillin[c]	amphotericin B[c]	capsofungin[c]
S. aureus	4[c]	2				
S. aureus (methicillin-res.)	4[c]		1			
S. aureus (multidrug-res.)	4[c]		1			
En. faecium	8		0.5			
E. coli	>250			4		
P. aeruginosa	>250	32				
C. albicans	4				1	
C. albicans (fluconazole-res.)	4				1	
C. auris	8					0.5
Cr. neoformans	16				2	

[a]Values are MIC in μg/mL, obtained from three independent experiments performed in duplicates. *S., Staphylococcus; En., Enterococcus; E., Escherichia; P., Pseudomonas; C., Candida; Cr., Cryptococcus.* [b]Average value over three independent trials with MIC ranging from 2 to 8 μg/mL. [c]Positive controls.

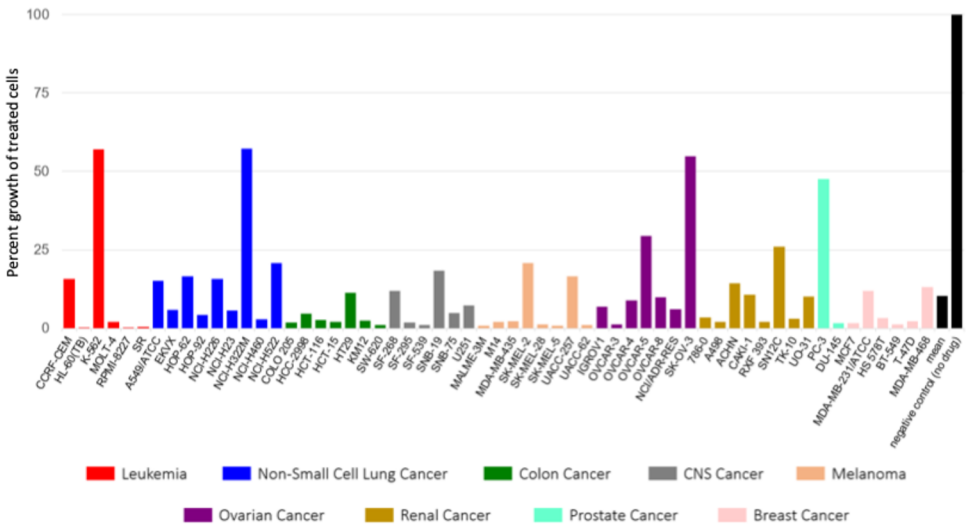

Figure 8. NCI one-dose 60-cell line panel screening of anthracaurisin A (**6**). Data are reported as a mean graph of the percent growth of treated cells with 10 μM anthracaurisin A (**6**). Growth is relative to the no-drug control and relative to the time zero number of cells. NCI identification number: NSC # D-856337/1; Experimental ID # 2507HT86.

Biological Activity

We tested anthracaurisin A's antimicrobial activity and cytotoxic potential *in vitro*, as well as its toxicity in zebrafish *in vivo*. For the antimicrobial assays, we tested a panel of human-pathogenic Gram-positive bacteria (*Staphylococcus* and *Enterococcus* spp.), Gram-negative bacteria (*Escherichia* and *Pseudomonas* spp.), and fungi (*Candida* and *Cryptococcus* spp.). Anthracaurisin A displayed significant antimicrobial activity against the Gram-positive bacteria and the fungi, with MIC values comprised between 4 μg/mL (7.2 μM) and 8 μg/mL (14.4 μM). No

https://doi.org/10.1021/acs.jnatprod.6c00531
J. Nat. Prod. 2026, 89, 1995−2007

activity against the selected Gram-negative bacteria was observed (Table 3).

Cytotoxic activity on cancer cells was evaluated via the NCI-60 cell line panel screening at a one dose concentration of 10 μM. In the presence of anthracaurisin A, all cell lines exhibited considerable growth reduction, with percentage growth ranging from 0.25% (cell line HL-60(TB)) to 57.19% (cell line NCI-H322M) compared to the negative control (no drug, 100% growth). Average growth of the cell line panel was 10.3%, demonstrating the broad-spectrum cytotoxic activity of anthracaurisin A against various cancer cell lines (Figure 8). This was further corroborated by our in-house MTT-based cell viability assay using HCT-116 (colon carcinoma), MCF-7 (breast adenocarcinoma), and PC3 (prostate adenocarcinoma) cancer cell lines. Against these cells, IC_{50} values of 0.3, 2.3, and 0.5 μM of **6** were established (Table 4). Lastly, the *in vivo* effects of anthracaurisin A were examined using a zebrafish embryo acute toxicity, yielding an LC_{50} value of 8.6 μM, similar to other mycotoxins discovered by our team (Figure 9).[16] Overall, anthracaurisin A has broad cytotoxic activity in the lower micromolar range and exhibits more potency than its aurisin congeners.[8,38] Future studies on its cellular mode of action are underway. Noteworthy, the monomer illudin S and its derivatives are potent DNA alkylating agents and completed a phase II clinical trial in late 2022 for oncology application (NCT03643107).[50,51]

Table 4. Cytotoxic Activity of Compound 6 against Various Cancer Cell Lines (IC_{50}, μM)[a,b]

mammalian cell line	6	mensacarcin[b]
HCT-116 (human colon carcinoma)	0.3 ± 0.1	2.7 ± 1.5
MCF-7 (human breast cancer)	2.3 ± 0.7	1.9 ± 1.1
PC3 (human prostate cancer)	0.5 ± 0.2	1.4 ± 0.5

[a]Values are mean IC_{50} ± standard deviations in μM, obtained from three independent experiments performed in triplicate. [b]Positive control.

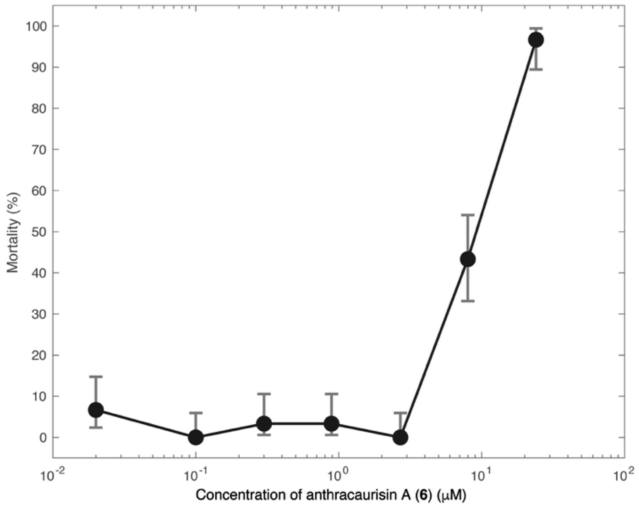

Figure 9. *In vivo* toxicity of anthracaurisin A (**6**) in zebrafish assay. Mortality dose–response curve for anthracaurisin A (**6**) in zebrafish embryo acute toxicity assay (LC_{50}= 8.6 ± 3 μM, n = 30).

EXPERIMENTAL SECTION

General Experimental Procedures

Illudin M (**1**), illudin S (**3**), and anthracaurisin A (**6**) 1D and 2D NMR spectra were recorded at 500 MHz for ^{1}H NMR and 125 MHz for ^{13}C NMR at 298 K on a Bruker Ascend 500 instrument equipped with a 5 mm probe (Bruker Corporation, Billerica, MA, USA). Chloroform-*d* was used for illudin M and anthracaurisin A and methanol-d_4 for illudin S. Using the same instrument, 1D and 2D ^{1}H and ^{13}C NMR spectra under increasing temperature of 323, 348, and 373 K were recorded for anthracaurisin A in dimethyl sulfoxide-d_6. Illudin B (**2**), 15-*O*-acetylilludin S (**4**), and dichomitin A (**5**) 1D and 2D NMR spectra were recorded at 600 MHz for ^{1}H NMR and 150 MHz for ^{13}C NMR at 298 K on a Bruker Avance Neo instrument equipped with a 1.7 mm TCI Micro CryoProbe in methanol-d_4. Solvents were used as internal standards and referenced as follows: δ_H 7.26 ppm, δ_C 77.16 ppm for chloroform-*d*; δ_H 3.31 ppm, δ_C 49.00 for methanol-d_4 and δ_H 2.50 ppm, δ_C 39.52 for dimethyl sulfoxide-d_6.[52] Optical rotations were measured on a JASCO P-2000 polarimeter at the sodium D line (589 nm), and they were averaged over ten integration periods (JASCO Applied Sciences, Halifax, Canada). We did not establish the enantiomeric excess or purity of **1**–**6** via chiral chromatography, as most natural products are made entiopure.[53] Therefore, we cannot exclude that these compounds exist as scalemic mixtures.

IR spectra were acquired on a Bruker α II FTIR spectrophotometer, and UV spectra were acquired using a Thermo Scientific Evolution 220 UV–visible spectrophotometer. VCD spectra were acquired in chloroform-*d* with a ChiralIR 2X Dual PEM FT-VCD spectrometer, set to 4 cm^{-1} resolution, with PEM (both 1 and 2) maximum frequency set to 1400 cm^{-1} (BioTools Inc., Jupiter, FL, USA). ECD spectra were acquired in acetonitrile using a Chirascan V100 instrument (Applied Photophysics, Leatherhead, England) in three trials at 1 s per step, and the results were averaged. Low-resolution LC-MS experiments were conducted on an Agilent 1100 series HPLC coupled to an Agilent 6130 Quadrupole LC/MS mass spectrometer with an electrospray ionization (ESI) source (Agilent Technologies, Santa Clara, CA, USA). Chromatography was performed using a Kinetex C_{18} column (150 mm × 4.6 mm, 5 μm, 100 Å, Phenomenex, Torrance, CA, USA), the oven was turned off, and the sample injection volume was 10–20 μL. A binary gradient consisting of water (eluent A) and acetonitrile (eluent B) (both +0.05% formic acid (FA)) at a constant flow rate of 800 μL/min was used. The gradient was applied as follows: 0–2 min, 10% B; 35 min, 100% B; 38 min, 100% B; 40 min, 10% B; 42 min, 10% B. For data acquisition and subsequent qualitative analysis, Agilent ChemStation software was used. High-resolution LC-MS and LC-MS/MS experiments were conducted on an Agilent 1290 Infinity II series UPLC coupled to an Agilent 6546 Q-TOF mass spectrometer with an electrospray ionization (Jet Stream ESI) source. Liquid chromatography was performed using a Kinetex C_{18} column (50 mm × 2.1 mm, 2.6 μm, 100 Å, Phenomenex, Torrance, CA, USA), the oven temperature was set to 40 °C, and the sample injection volume was 3–5 μL. A binary gradient consisting of water (eluent A) and acetonitrile (eluent B) (both +0.05% FA) at a constant flow rate of 400 μL/min was used. The gradient was applied as follows: 0–0.25 min, 10% B; 10.00 min, 95% B; 13.00 min, 95% B; 13.1 min, 10% B; 15.00 min, 10% B. For data acquisition and subsequent qualitative analysis, Agilent MassHunter software was used. Preparative HPLC experiments were carried out on an Agilent 1260 Infinity II series apparatus exhibiting a Luna C_{18} column (AXIA, New Column 250 mm × 21.1 mm, 5 μm, 100 Å, Phenomenex, Torrance, CA, USA). Semipreparative HPLC experiments were performed on an Agilent 1100 series apparatus equipped with a Luna C_{18} column (AXIA, New Column 250 mm × 10 mm, 5 μm, 100 Å, Phenomenex, Torrance, CA, USA). Fungal genomic DNA for barcoding experiments was extracted using the DNeasy Blood and Tissue Kit (Qiagen, Germantown, MD, USA). PCR was performed in a MyCycler thermal cycler (Bio-Rad Laboratories Inc., Hercules, CA, USA). PCR products were submitted to DNA gel electrophoresis in 1% agarose gel in the presence of GelRed nucleic acid stain (Biotium Inc., Fremont, CA, USA) and visualized using a Bio-Rad UV Transilluminator 2000 or an Azure Gel Imager 400

https://doi.org/10.1021/acs.jnatprod.6c00531
J. Nat. Prod. 2026, 89, 1995–2007

(Azure Biosystems, Dublin, CA, USA). All solvents were purchased from Thermo Fisher (Thermo Fisher Scientific Inc., Waltham, MA, USA) or VWR (VWR International, Radnor, PA, USA).

Fungal Strain Collection and Identification

The fungus was found on dead indeterminate branches at Fundo La Cantera y El Guindo, Concepción, Biobío Region, Chile (−36.837173° S, −73.025636° W) and collected in August 2019. It was later identified as *A. discolor* based on morphological features. A voucher specimen (VALD-F 0003) has been deposited in the VALDF herbarium of the Universidad Austral de Chile in Valdivia, Chile. To further identify the species by genomic tools, its ITS was sequenced. Briefly, a small culture of the fungus was grown for 3 weeks in 125 mL liquid malt-based medium. The mycelium was collected, and genomic DNA was extracted using the DNeasy Blood and Tissue Kit from Qiagen following the manufacturer's guidelines. The ITS region was amplified by PCR using primers ITS1 and ITS4[54] in association with the commercial master mix MangoMix (Meridian Bioscience, Cincinnati, OH, USA). Resulting amplicons were then sequenced by Sanger sequencing (Azenta Life Science, South Plainfield, NJ, USA). In total, eight ITS sequences were retrieved, each originating from an independent replicate of DNA extraction. All sequences were pairwise aligned with the reference databases FunCBS, EF1, ITS, Unite, Mycokey, fusarioidID, Morchella, PasteurYeasts, PasteurMOLDS, and MIRRI in MycoBank. All sequences aligned with *Anthracophyllum* spp. sequences, sometimes specified to *A. archeri* or *A. lateritium*. Out of the eight sequences aligned with the databases, four showed a similarity score of 94% or above with at least one *Anthracophyllum* sp. (Figure S65).

Fermentation, Extraction, and Isolation

The fungus was grown in two 500 mL glass mason jars filled with autoclaved rice medium (50% v/v rice to 50% v/v DI water) for 4 weeks without shaking. After this period of fermentation, the jars were extracted with ethyl acetate by maceration and manual stirring followed by filtration through a paper filter. The resulting liquid was concentrated *in vacuo* to obtain the organic extract (974 mg). A portion of this extract (200 mg) was subjected to preparative HPLC applying an acetonitrile/water gradient from 10 to 50% acetonitrile in 35 min, followed by a 98% acetonitrile wash for 10 min, on a Phenomenex Luna column (C_{18}(2), 5 μm, 100 Å, AXIA, 250 mm × 21.1 mm) at a flow rate of 28.32 mL/min. Compound **1** (3.6 mg (yield 18.0 mg/L), R_t 23.6 min), **2** (0.5 mg (yield 2.5 mg/L), R_t 15.9 min), **3** (6.0 mg (yield 30.0 mg/L), R_t 11.1 min), **6** (30.0 mg (yield 150.0 mg/L), R_t 39.2 min), and a mixture of **4** and **5** (3.0 mg, R_t 20.7 min) were isolated. The later was further purified by semipreparative HPLC employing an acetonitrile/water gradient composed of 20% isocratic acetonitrile for 35 min, followed by a 98% acetonitrile wash for 7 min, on a Phenomenex Luna column (C_{18}(2), 5 μm, 100 Å, AXIA, 250 mm × 10 mm) at a flow rate of 5.0 mL/min. This experiment allowed the isolation of compound **4** (1.3 mg (yield 6.5 mg/L), R_t 26.2 min) and **5** (1.8 mg (yield 9.0 mg/L), R_t 33.4 min).

15-*O*-acetylilludin S (**4**): yellowish oil; $[\alpha]_D^{22}$ −80° (*c* 0.1, MeOH); UV/vis (MeOH) λ_{max} (log ε) 203.4 (3.87), 222.4 (3.95), 316.0 (3.31) nm (Figure S10); ECD (acetonitrile) λ_{max} ($\Delta\varepsilon$) 216 (+64.6), 249 (−36.6), 271 (−2.2), 340 (−7.5) nm; IR ν_{max} 3457, 2939, 1700, 1609, 1375, 1237, 1107, 1032, 945, 825, 764 cm^{-1} (Figure S9); ^{1}H and ^{13}C NMR (Table 1); ESIMS *m*/*z* 351.1 [M + FA−H]$^-$, *m*/*z* 341.1 [M + Cl]$^-$, *m*/*z* 289.1 [M−H_2O + H]$^+$, *m*/*z* 307.1 [M + H]$^+$, *m*/*z* 324.1 [M + NH_4]$^+$, *m*/*z* 635.3 [2M + Na]$^+$ (Figure S7); HRESIMS *m*/*z* 245.1192 [M−acetyl−H_2O−H]$^-$ (calcd for $C_{15}H_{17}O_3^-$, 245.1183), *m*/*z* 289.1435 [M−H_2O + H]$^+$ (calcd for $C_{17}H_{21}O_4^+$, 289.1434), *m*/*z* 329.1361 [M + Na]$^+$ (calcd for $C_{17}H_{22}O_5Na^+$, 329.1359) (Figure S8).

Anthracaurisin A (**6**): yellowish oil; $[\alpha]_D^{22}$ +64° (*c* 0.1, MeOH), +76° (*c* 0.1, $CHCl_3$); UV/vis (MeOH) λ_{max} (log ε) 201.3 (3.77), 286.0 (4.15) nm (Figure S45); ECD (acetonitrile) λ_{max} ($\Delta\varepsilon$) 185 (+11.4), 217 (+0.5), 279 (+15.0), 318 (−6.1) nm; IR ν_{max} 2967, 1751, 1683, 1619, 1462, 1373, 1226, 1179, 1133, 1027, 935, 861, 795 cm^{-1} (Figure S44); ^{1}H and ^{13}C NMR (Tables 2, S37, and S47); ESIMS *m*/*z* 553.2 [M−H]$^-$, *m*/*z* 495.2 [M−acetyl−H_2O + H]$^+$, *m*/*z* 435.2 [M−2acetyl−2H_2O + H]$^+$ (Figure S40); HRESIMS *m*/*z* 553.2831 [M−H]$^-$ (calcd for $C_{32}H_{41}O_8^-$, 553.2807), *m*/*z* 575.2643 [M + Na−2H]$^-$ (calcd for $C_{32}H_{40}O_8Na^-$, 575.2626), *m*/*z* 511.2714 [M−acetyl−H]$^-$ (calcd for $C_{30}H_{39}O_7^-$, 511.2701), *m*/*z* 493.2601 [M−acetyl−H_2O−H]$^-$ (calcd for $C_{30}H_{37}O_6^-$, 493.2596) (Figure S41).

VCD and ECD Measurements and Computations

Compounds subjected to VCD analyses were solubilized in chloroform-*d*, which was run through a small plug of activated basic alumina immediately before use. The resulting solution was transferred to a liquid IR cell (BaF_2, 100 μm cell path) and placed in the measurement chamber. The VCD was then acquired (BioTools Inc. ChiralIR 2X Dual PEM FT-VCD spectrometer) at 4 cm^{-1} resolution, with PEM (both 1 and 2) maximum frequency set to 1400 cm^{-1}. The sample was measured for several hours in 1 h blocks. The IR data from the first block were solvent and water vapor subtracted and then offset to zero at 2000 cm^{-1}. The VCD data blocks were averaged, and from this was subtracted a previously measured solvent baseline. Finally, the VCD spectrum was offset to zero at 2000 cm^{-1}. The VCD noise data was block averaged and used without further processing. Compounds subjected to ECD measurements were solubilized in acetonitrile and transferred to a 500 μm UV−vis cell. The absorbance was checked, and the solution was diluted until an absorbance of 0.8 was achieved for the UV−vis max absorbance (285 nm). The UV−vis and ECD spectra were then acquired (Applied Photophysics Chirascan V100 spectrometer) in three trials at 1 s per step, and the results were averaged. The solvent was measured under the same conditions and was used to correct both the UV−vis and ECD spectra. For each compound, the different candidate stereoisomers were constructed using ComputeVOA (BioTools, Jupiter, FL, USA). A thorough conformational search was performed at the MM level using the MMF94 force field in a 7 kcal/mol energy window. The conformers found were subjected to DFT level optimization and frequency calculation with Gaussian '09 (Gaussian Inc., Wallingford, CT, USA) using the B3LYP/6−31G(d) and B3PW91/6−31G(d) methods.[55] The resulting lowest energy unique conformations were reoptimized using the B3LYP/cc-pVTZ and B3PW91/cc-pVTZ methods, and the IR and VCD frequencies recalculated at these levels. The resulting spectra from all methods were Boltzmann averaged (using both free energy and electronic energy), plotted at 5 cm^{-1} resolution, and then uniformly *x*-axis scaled (values obtained using CompareVOA and varied with basis set and functional from 0.968 to 0.984) for comparison to the experimental IR and VCD spectra. The two different weighing methods (free energy and electronic energy) were compared to the experimental data. The same approach was applied to each of the alternate structures, and the same method was used to produce spectra for these stereoisomers. The B3PW91/cc-pVTZ calculations gave the best match to the experiment and are used in all plots and comparisons. The optimized structures of conformers obtained from the VCD calculation were subjected to UV−vis/ECD calculation using the TD-DFT method in Gaussian '09 at the CAM-B3LYP/TZVP level for 200 excited states.[55] The results were Boltzmann averaged using free energy and plotted at 0.333 eV HWHH and then uniformly scaled for comparison to the experiment.

Cell Culture Assays

Colon cancer (HCT-116), breast adenocarcinoma (MCF-7), and prostate adenocarcinoma (PC-3) cells were purchased from the American Type Culture Collection (ATCC, Manassas, VA, USA). Dulbecco's modified Eagle's medium (DMEM), RPMI 1640, phosphate-buffered saline (PBS), trypsin/EDTA (0.25%/2.21 mM), and penicillin/streptomycin solution were obtained from Thermo Fisher Scientific. Fetal bovine serum (FBS) was obtained from R&D systems. HCT-116 and MCF-7 cells were cultivated in DMEM and PC-3 cells in RPMI 1640, each supplemented with 10% (v/v) fetal bovine serum, penicillin (100 U/mL), and streptomycin (100 μg/mL). The cell lines were incubated at 37 °C, 5% CO_2. Cells were plated into 96-well plates at different densities (HCT-116:7000 cells/well; PC3:7000 cells/well, MF7:9000 cells/well). The passage number for cells used in the experiments never exceeded 15. All cell lines were tested mycoplasma-negative by real-time PCR (Myco Solutions mycoplasma detection kit, Akron Biotech, Boca Raton, FL, USA). Growth inhibition and cytotoxicity in the different cell lines were measured by the reduction of the tetrazolium salt MTT by metabolically active cells.[56]

https://doi.org/10.1021/acs.jnatprod.6c00531
J. Nat. Prod. 2026, 89, 1995−2007

Cells were plated into 96-well plates and maintained overnight before treatment was started with the addition of mensacarcin to each well. After the designated time, MTT (5 mg/mL in PBS) was added to each well at a final concentration of 0.5 mg/mL. The plates were incubated for 2 h at 37 °C. The medium was removed, cells were lysed, and the purple formazan product was solubilized by the addition of 50 μL of DMSO. Absorbance was measured at 550 nm with a microplate reader (Synergy HTX, Biotek, Winooski, VT, USA). Metabolic activity of vehicle-treated cells (0.5% DMSO unless otherwise stated) was defined as 100% cell growth.

Antimicrobial Assays

For antibacterial activity in cell-based assays, established protocols were followed.[57,58] Gram-positive bacteria, including *Enterococcus faecium* (ATCC 49032), *Staphylococcus aureus* (ATCC 25923), methicillin-resistant *S. aureus* (ATCC BAA-41), and multidrug-resistant *S. aureus* (ATCC BAA44), two Gram-negative pathogens, *Pseudomonas aeruginosa* (ATCC 15442) and *Escherichia coli* (ATCC 8739), as well as several fungi such as *Candida albicans* (ATCC 90027), fluconazole-resistant *C. albicans* (ATCC 10231), *Cryptococcus neoformans* (ATCC 14116), and *C. auris* (CDC B11903) were tested. Vancomycin, kanamycin, ampicillin, amphotericin B, fluconazole, and caspofungin were used as positive controls. DMSO served as the negative control. MICs were determined based on two independent experiments performed in duplicates.[57] For the single-dose assay, compounds, mixtures, and antibiotic controls were tested at 125 μg/mL. Microbial growth rates were measured after 16 h by absorbance at 620 nm using a Biotek Synergy 96-well plate reader (BioTek, Winooski, VT, USA). All human pathogens used in the study were acquired from the ATCC.

Zebrafish Assay *In Vivo* Toxicity

Zebrafish adults (*Danio rerio*, AB strain) were reared under standard conditions (28 °C, 14:10 light:dark) and crossed to produce embryos. Embryos with intact chorions were transferred into 96-well plates (1 embryo/well) at 24 h postfertilization (hpf) using 50 μL of medium (HEPES-buffered E3:5 mM NaCl, 0.17 mM KCl, 0.33 mM $CaCl_2$, 0.33 mM $MgSO_4$, 1 mM HEPES, titrated to 7.2 pH). Compound **6** was dissolved in DMSO, serially diluted using HEPES-buffered E3, and then added to well plates (final conc.: 0, 2.0, 5.0, 15, 25, and 50 μM in 1% DMSO). Plates were incubated for 48 h (72 hpf; 28 °C, 14:10 light:dark), after which the number of surviving embryos was counted. Each assay examined eight embryos per concentration, and the assay was replicated three times using animals from three clutches. The results were similar across replicates, and so survivorship is plotted from pooled data, with error bars representing 68% confidence intervals (like SEM) found by fitting results for each concentration to a binomial distribution (MATLAB R2020b). EC_{50} values were calculated by fitting unpooled survivorship values to the Hill equation, and 95% confidence intervals were calculated using a bootstrap analysis. Protocols were approved by the University of Florida's Institutional Animal Care and Use Committee.[16]

■ ASSOCIATED CONTENT

Data Availability Statement

The NMR raw data files for compounds **1**–**6** have been deposited to the NIH Natural Products Magnetic Resonance Database (NP-MRD)[59] (https://np-mrd.org) under NP-CARD: NP0139324 (**1**), NP-CARD: NP0353957 (**2**), NP-CARD: NP0004898 (**3**), NP-CARD: NP0353958 (**4**), NP-CARD: NP0353959 (**5**), NP-CARD: NP0353960 (**6**), and Natural Products Atlas.[19] Anthracaurisin A derived MS/MS spectra have been added to the GNPS Public Spectral Library.

Supporting Information

The Supporting Information is available free of charge at https://pubs.acs.org/doi/10.1021/acs.jnatprod.6c00531.

NMR, MS, UV−vis, IR, and CD spectra of compounds; DFT calculation details and coordinates; ITS sequences; note on carbon numbering systems for illudins (PDF)

■ AUTHOR INFORMATION

Corresponding Author

Sandra Loesgen − *Department of Chemistry, Whitney Laboratory for Marine Bioscience, University of Florida, St. Augustine, Florida 32080, United States;* orcid.org/0000-0003-1090-564X; Email: sandra.loesgen@ufl.edu

Authors

Bastien Petit − *Department of Chemistry, Whitney Laboratory for Marine Bioscience, University of Florida, St. Augustine, Florida 32080, United States*

Ines Michrafy − *Department of Chemistry, Whitney Laboratory for Marine Bioscience, University of Florida, St. Augustine, Florida 32080, United States;* orcid.org/0009-0001-9776-743X

Jordan Nafie − *BioTools Inc., Florida 33407, United States;* orcid.org/0000-0003-1986-0302

Grayce E. Dyer − *Department of Chemistry, Whitney Laboratory for Marine Bioscience, University of Florida, St. Augustine, Florida 32080, United States;* orcid.org/0009-0007-8309-1487

Erin M. Marshall − *Department of Chemistry, Whitney Laboratory for Marine Bioscience, University of Florida, St. Augustine, Florida 32080, United States*

Cristian Riquelme − *Departamento de Química, Laboratorio de Química Aplicada y Sustentable (LabQAS), Universidad del Bío-Bío, Concepción 4051381, Chile;* orcid.org/0000-0003-1652-571X

Jaime R. Cabrera-Pardo − *Departamento de Química, Laboratorio de Química Aplicada y Sustentable (LabQAS), Universidad del Bío-Bío, Concepción 4051381, Chile; College of Dental Medicine, Roseman University of Health Sciences, South Jordan, Utah 84095, United States;* orcid.org/0000-0001-6978-581X

James A. Strother − *Department of Biology, Whitney Laboratory for Marine Bioscience, University of Florida, St. Augustine, Florida 32080, United States;* orcid.org/0000-0001-6871-5561

Complete contact information is available at: https://pubs.acs.org/10.1021/acs.jnatprod.6c00531

Notes

The authors declare no competing financial interest.

■ ACKNOWLEDGMENTS

We wish to thank Sam Xia (UNF), James Rocca (UF), and Ying Li (UF, AMRIS) for excellent NMR support. The National High Magnetic Field Laboratory's Advanced Magnetic Resonance Imaging and Spectroscopy (AMRIS) Facility is supported by the National Science Foundation Cooperative Agreement DMR-1644779 and the State of Florida, and we are grateful for NHMFL user grants. We wish to thank the National Cancer Institute Developmental Therapeutics Program (NCI/DTP) (https://cancer.gov/programs/dtp) for providing NCI-60 panel data for compound **6** (NSC # D-856337/1; Experimental ID # 2507HT86). We also thank Lucas Cathey, Zain Khalid, Lydia Mayhood, and Emily Lekas for assistance with zebrafish care. We like to thank Mario Rajchenberg for his input on fungal

taxonomy and Valentina Parada for her help with the isolation of the fungus. We thank Profs. Jeff Rudolf (UF), Joe Ryan (UF), and Paul Blakemore (OSU) for fruitful discussions. This work was supported by NSF CH-2020110 (S.L.). S.L. is grateful for UF Start-Up funds.

REFERENCES

(1) Riedling, O. L.; Rokas, A. mGem: How Many Fungal Secondary Metabolites Are Produced by Filamentous Fungi? Conservatively, at Least 1.4 Million. *mBio* **2025**, *16* (10), No. e01381−25.
(2) Rokas, A.; Mead, M. E.; Steenwyk, J. L.; Raja, H. A.; Oberlies, N. H. Biosynthetic Gene Clusters and the Evolution of Fungal Chemodiversity. *Nat. Prod. Rep.* **2020**, *37* (7), 868−878.
(3) Lin, H.-C.; Hewage, R. T.; Lu, Y.-C.; Chooi, Y.-H. Biosynthesis of Bioactive Natural Products from Basidiomycota. *Org. Biomol. Chem.* **2019**, *17* (5), 1027−1036.
(4) Schäfer, T.; Haun, F.; Rupp, B.; Hoffmeister, D. Dissimilar Reactions and Enzymes for Psilocybin Biosynthesis in Inocybe and Psilocybe Mushrooms. *Angew. Chem., Int. Ed.* **2025**, *64* (46), No. e202512017.
(5) Banki, O.; Hobern, D.; Döring, M.; Ower, G.; Roskov, Y.; Hernandez-Robles, D.; et al. Towards a Quality Assurance and Quality Control Mechanism for Species List Building. *Biodiversity Inf. Sci. Stand.* **2023**, *7*, No. e111665.
(6) Nguyen, T. T.; Do, H. H.; Nguyen-Sy, T.; Huynh, U. T. D.; Hai, N. T. L.; Phan, T. T. T.; Nguyen, T. T. H.; Khang, D. T.; Tran, P. T. *Anthracophyllum sontraense* (Omphalotaceae, Agaricales), A New Species from Danang, Vietnam. *Mycobiology* **2024**, *52* (6), 454−463.
(7) Yang, W.-J.; Xu, M.; Zhang, J.; Zhou, F.; Le, Z.-F.; Tong, W.-J.; Song, H.-Y.; Jin, Z.-H.; Cheng, Q.-G.; Zhou, J.-P.; Gao, Y.; Zhai, Z.-J.; Hu, H.-J.; Chen, M.-H.; Yin, H.; Wang, J.; Hu, D.-M. Morphological and Phylogenetic Analyses Reveal a New Species of Anthracophyllum (Omphalotaceae, Agaricales) in Zhejiang Province, China. *Arch. Microbiol.* **2024**, *206* (2), No. 63.
(8) Intaraudom, C.; Boonyuen, N.; Supothina, S.; Tobwor, P.; Prabpai, S.; Kongsaeree, P.; Pittayakhajonwut, P. Novel Spiro-Sesquiterpene from the Mushroom *Anthracophyllum* Sp. BCC18695. *Phytochem. Lett.* **2013**, *6* (3), 345−349.
(9) Fernando, D. M.; Wijesundera, R. L. C.; Soysa, P.; de Silva, D.; Nanayakkara, C. M. Antioxidant Potential, in Vitro Cytotoxicity and Apoptotic Effect Induced by Crude Organic Extract of Anthracophyllum Lateritium against RD Sarcoma Cells. *BMC Complementary Altern. Med.* **2015**, *15*, No. 398.
(10) Jägers, E.; Hillen-Maske, E.; Schmidt, H.; Steglich, W.; Horak, E. Pilzfarbstoffe, 55 [1]/Fungal Pigments, 55 [1]: Acetylierte Terphenylchinon-Derivate Aus Anthracophyllum-Arten (Agaricales) /. *Z. Naturforsch., B* **1987**, *42* (10), 1354−1360.
(11) Liu, J.-K. Natural Terphenyls: Developments since 1877. *Chem. Rev.* **2006**, *106* (6), 2209−2223.
(12) Cea, M.; Jorquera, M.; Rubilar, O.; Langer, H.; Tortella, G.; Diez, M. C. Bioremediation of Soil Contaminated with Pentachlorophenol by Anthracophyllum Discolor and Its Effect on Soil Microbial Community. *J. Hazard. Mater.* **2010**, *181* (1−3), 315−323.
(13) Acevedo, F.; Pizzul, L.; Castillo, M. d. P.; Cuevas, R.; Diez, M. C. Degradation of Polycyclic Aromatic Hydrocarbons by the Chilean White-Rot Fungus *Anthracophyllum discolor*. *J. Hazard. Mater.* **2011**, *185* (1), 212−219.
(14) Elgueta, S.; Santos, C.; Lima, N.; Diez, M. C. Immobilization of the White-Rot Fungus Anthracophyllum Discolor to Degrade the Herbicide Atrazine. *AMB Express* **2016**, *6*, No. 104.
(15) Benavides, V.; Pinto-Ibieta, F.; Serrano, A.; Rubilar, O.; Ciudad, G. Use of Anthracophyllum Discolor and Stereum Hirsutum as a Suitable Strategy for Delignification and Phenolic Removal of Olive Mill Solid Waste. *Foods* **2022**, *11* (11), No. 1587.
(16) Jagels, A.; Adpressa, D. A.; Kaweesa, E. N.; McCauley, M.; Philmus, B.; Strother, J. A.; Loesgen, S. Metabolomics-Guided Discovery, Isolation, Structure Elucidation, and Bioactivity of Myropeptins C−E from *Myrothecium inundatum*. *J. Nat. Prod.* **2023**, *86* (7), 1723−1735.
(17) Bunnell, A. A.; Marshall, E. M.; Estes, S. K.; Deadmond, M. C.; Loesgen, S.; Strother, J. A. Embryonic Zebrafish Irritant-Evoked Hyperlocomotion (EZIH) as a High-Throughput Behavioral Model for Nociception. *Behav. Brain Res.* **2025**, *485*, No. 115526.
(18) Blunt, J.; Munro, M.; Laatsch, H. *AntiMarin Database*; University of Canterbury: 2006.
(19) Poynton, E. F.; van Santen, J. A.; Pin, M.; Contreras, M. M.; McMann, E.; Parra, J.; Showalter, B.; Zaroubi, L.; Duncan, K. R.; Linington, R. G. The Natural Products Atlas 3.0: Extending the Database of Microbially Derived Natural Products. *Nucleic Acids Res.* **2025**, *53*, D691−D699.
(20) McMorris, T. C.; Kelner, M. J.; Chadha, R. K.; Siegel, J. S.; Moon, S.; Moya, M. M. Structure and Reactivity of Illudins. *Tetrahedron* **1989**, *45* (17), 5433−5440.
(21) McMorris, T. C.; Anchel, M. Fungal Metabolites. The Structures of the Novel Sesquiterpenoids Illudin-S and -M. *J. Am. Chem. Soc.* **1965**, *87* (7), 1594−1600.
(22) Nord, C.; Menkis, A.; Broberg, A. Cytotoxic Illudane Sesquiterpenes from the Fungus Granulobasidium Vellereum (Ellis and Cragin) Jülich. *J. Nat. Prod.* **2015**, *78* (11), 2559−2564.
(23) Aoki, S.; Aboshi, T.; Shiono, Y.; Kimura, K.-I.; Murata, T.; Arai, D.; Iizuka, Y.; Murayama, T. Constituents of the Fruiting Body of Poisonous Mushroom Omphalotus Japonicus. *Chem. Pharm. Bull.* **2020**, *68* (5), 436−442.
(24) Dai, Q.; Zhang, F.-L.; Du, J.-X.; Li, Z.-H.; Feng, T.; Liu, J.-K. Illudane Sesquiterpenoids from Edible Mushroom Agrocybe Salicacola and Their Bioactivities. *ACS Omega* **2020**, *5* (34), 21961−21967.
(25) Kanehara, R.; Tonouchi, A.; Konno, K.; Koshino, H.; Hashimoto, M. Isolation of Cyclohumulanoids from *Daedaleopsis tricolor* and Their Biosynthesis Based on *in Silico* Simulations. *Tetrahedron* **2022**, *123*, No. 133006.
(26) Du, J.-X.; Li, X.-M.; Yang, H.-X.; Teng, S.-Q.; Liu, J.-K.; Feng, T. Phellinilludins A−D, New Illudane Sesquiterpenes from the Fungus *Phellinus tremulae*. *Phytochem. Lett.* **2023**, *54*, 86−90.
(27) Arnone, A.; Cardillo, R.; Nasini, G.; Pava, O. V. d. Secondary Mould Metabolites. Part 31. Isolation and Structure Elucidation of Illudins A and B, and Illudalenol, New Sesquiterpenoids from Clitocybe Illudens. *J. Chem. Soc. Perkin 1* **1991**, *4*, 733−737.
(28) Burgess, M. L.; Zhang, Y. L.; Barrow, K. D. Characterization of New Illudanes, Illudins F, G, and H from the Basidiomycete Omphalotus Nidiformis. *J. Nat. Prod.* **1999**, *62* (11), 1542−1544.
(29) Intra, A.; Bava, A.; Nasini, G.; Riva, S. Regioselective Enzymatic Acylation of Polyhydroxylated Sesquiterpenoids. *J. Mol. Catal. B: Enzym.* **2004**, *29* (1), 95−98.
(30) McMorris, T. C.; Kelner, M. J.; Wang, W.; Estes, L. A.; Montoya, M. A.; Taetle, R. Structure-Activity Relationships of Illudins: Analogs with Improved Therapeutic Index. *J. Org. Chem.* **1992**, *57* (25), 6876−6883.
(31) Huang, Z.; Dan, Y.; Huang, Y.; Lin, L.; Li, T.; Ye, W.; Wei, X. Sesquiterpenes from the Mycelial Cultures of Dichomitus Squalens. *J. Nat. Prod.* **2004**, *67* (12), 2121−2123.
(32) Xie, H.-H.; Xu, X.-Y.; Dan, Y.; Wei, X.-Y. Novel Sesquiterpenes from the Mycelial Cultures of Dichomitus Squalens. *Helv. Chim. Acta* **2011**, *94* (5), 868−874.
(33) Keller, P. A.; Butler, N. M.; McCosker, P. M. Axially Chiral Natural Products and Bioactive Compounds. In *Atropisomerism and Axial Chirality*; World Scientific (Europe), 2019; pp 611−656 DOI: 10.1142/9781786346469_0009.
(34) LaPlante, S. R.; Edwards, P. J.; Fader, L. D.; Jakalian, A.; Hucke, O. Revealing Atropisomer Axial Chirality in Drug Discovery. *ChemMedChem* **2011**, *6* (3), 505−513.
(35) He, Y.; Bo, W.; Dukor, R. K.; Nafie, L. A. Determination of Absolute Configuration of Chiral Molecules Using Vibrational Optical Activity: A Review. *Appl. Spectrosc.* **2011**, *65* (7), 699−723.
(36) Debie, E.; De Gussem, E.; Dukor, R. K.; Herrebout, W.; Nafie, L. A.; Bultinck, P. A Confidence Level Algorithm for the Determination of

https://doi.org/10.1021/acs.jnatprod.6c00531
J. Nat. Prod. 2026, 89, 1995−2007

Absolute Configuration Using Vibrational Circular Dichroism or Raman Optical Activity. *ChemPhysChem* **2011**, *12* (8), 1542−1549.
(37) Boehlendorf, B.; Neff, S.; Schuez, T. C.; Molleyres, L.-P.; Winkler, T.; Dobler, M.; Huang, Y. Compounds Obtained from a Fungal Microorganism and Derivatives Thereof. U.K. Patent GB2,396,349A, 2004.
(38) Kanokmedhakul, S.; Lekphrom, R.; Kanokmedhakul, K.; Hahnvajanawong, C.; Bua-art, S.; Saksirirat, W.; Prabpai, S.; Kongsaeree, P. Cytotoxic Sesquiterpenes from Luminescent Mushroom *Neonothopanus nambi*. *Tetrahedron* **2012**, *68* (39), 8261−8266.
(39) Durán-Peña, M. J.; Ares, J. M. B.; Hanson, J. R.; Collado, I. G.; Hernández-Galán, R. Biological Activity of Natural Sesquiterpenoids Containing a Gem-Dimethylcyclopropane Unit. *Nat. Prod. Rep.* **2015**, *32* (8), 1236−1248.
(40) Kakumu, Y.; Chaudhri, A. A.; Helfrich, E. J. N. The Role and Mechanisms of Canonical and Non-Canonical Tailoring Enzymes in Bacterial Terpenoid Biosynthesis. *Nat. Prod. Rep.* **2025**, *42* (3), 501−539.
(41) Nett, R. S.; Dickschat, J. S.; Peters, R. J. Labeling Studies Clarify the Committed Step in Bacterial Gibberellin Biosynthesis. *Org. Lett.* **2016**, *18* (23), 5974−5977.
(42) Hsieh, C. H.; Huang, X.; Amaya, J. A.; Rutland, C. D.; Keys, C. L.; Groves, J. T.; Austin, R. N.; Makris, T. M. The Enigmatic P450 Decarboxylase OleT Is Capable of, but Evolved To Frustrate, Oxygen Rebound Chemistry. *Biochemistry* **2017**, *56* (26), 3347−3357.
(43) Han, Z.-z.; Ye, J.; Liu, Q.-X.; Shen, Y.; Yue, R.-C.; Li, H.-L.; Zhang, W.-D. Valeriadimers A−C, Three Sesquiterpenoid Dimers from Valeriana Officinalis Var. Latifolia. *RSC Adv.* **2015**, *5* (8), 5913−5916.
(44) Yamaguchi, Y.; Manita, D.; Takeuchi, T.; Kuramochi, K.; Kuriyama, I.; Sugawara, F.; Yoshida, H.; Mizushina, Y. Novel Terpenoids, Trichoderonic Acids A and B Isolated from Trichoderma Virens, Are Selective Inhibitors of Family X DNA Polymerases. *Biosci. Biotechnol. Biochem.* **2010**, *74* (4), 793−801.
(45) Liu, L.; Han, J.-J.; Xu, T.-S.; Liu, R.-X.; Bao, L.; Liu, H.-W. Three New Heptelidic Acid Derivatives from the Culture of Mushroom Lentinellus Ursinus. *Nat. Prod. Bioprospect.* **2018**, *8* (5), 355−360.
(46) Jiao, W.-H.; Dewapriya, P.; Mohamed, O.; Khalil, Z. G.; Salim, A. A.; Lin, H.-W.; Capon, R. J. Divirensols: Sesquiterpene Dimers from the Australian Termite Nest-Derived Fungus Trichoderma Virens CMB-TN16. *J. Nat. Prod.* **2019**, *82* (1), 87−95.
(47) Sun, L.-L.; Shao, C.-L.; Chen, J.-F.; Guo, Z.-Y.; Fu, X.-M.; Chen, M.; Chen, Y.-Y.; Li, R.; de Voogd, N. J.; She, Z.-G.; Lin, Y.-C.; Wang, C.-Y. New Bisabolane Sesquiterpenoids from a Marine-Derived Fungus Aspergillus Sp. Isolated from the Sponge Xestospongia Testudinaria. *Bioorg. Med. Chem. Lett.* **2012**, *22* (3), 1326−1329.
(48) de Vivar, A. R.; Delgado, G. Structure and Stereochemistry of Mexicanin F, a Novel Dimeric nor-Sesquiterpene Lactone from *Helenium mexicanum*. *Tetrahedron Lett.* **1985**, *26* (5), 579−582.
(49) Wu, H.-H.; Chen, Y.-P.; Ying, S.-S.; Zhang, P.; Xu, Y.-T.; Gao, X.-M.; Zhu, Y. Dinardokanshones A and B, Two Unique Sesquiterpene Dimers from the Roots and Rhizomes of *Nardostachys chinensis*. *Tetrahedron Lett.* **2015**, *56* (43), 5851−5854.
(50) Casimir, L.; Zimmer, S.; Racine-Brassard, F.; Jacques, P.-É.; Maréchal, A. The Mutational Impact of Illudin S on Human Cells. *DNA Repair* **2023**, *122*, No. 103433.
(51) Butler, M. S.; Capon, R. J.; Blaskovich, M. A. T.; Henderson, I. R. Natural Product-Derived Compounds in Clinical Trials and Drug Approvals. *Nat. Prod. Rep.* **2026**, *43*, 20−88.
(52) Fulmer, G. R.; Miller, A. J. M.; Sherden, N. H.; Gottlieb, H. E.; Nudelman, A.; Stoltz, B. M.; Bercaw, J. E.; Goldberg, K. I. NMR Chemical Shifts of Trace Impurities: Common Laboratory Solvents, Organics, and Gases in Deuterated Solvents Relevant to the Organometallic Chemist. *Organometallics* **2010**, *29* (9), 2176−2179.
(53) Mazzotta, S.; Rositano, V.; Senaldi, L.; Bernardi, A.; Allegrini, P.; Appendino, G. Scalemic Natural Products. *Nat. Prod. Rep.* **2023**, *40* (10), 1647−1671.
(54) White, T. J.; Bruns, T.; Lee, S.; Taylor, J. Amplification and Direct Sequencing Of Fungal Ribosomal Rna Genes For Phylogenetics. In *PCR Protocols*; Elsevier, 1990; pp 315−322 DOI: 10.1016/B978-0-12-372180-8.50042-1.
(55) Frisch, M. J.; Trucks, G. W.; Schlegel, H. B.et al. *Gaussian Revision 01*; Gaussian. Inc: Wallingford CT, 2009. https://cir.nii.ac.jp/crid/1370298757422456580.
(56) Riss, T. L.; Moravec, R. A.; Niles, A. L.; Duellman, S.; Benink, H. A.; Worzella, T. J.; Minor, L. Cell Viability Assays. In *Assay Guidance Manual*; Markossian, S.; Grossman, A.; Arkin, M.; Auld, D.; Austin, C.; Baell, J.; Brimacombe, K.; Chung, T. D. Y.; Coussens, N. P.; Dahlin, J. L.; Devanarayan, V.; Foley, T. L.; Glicksman, M.; Gorshkov, K.; Haas, J. V.; Hall, M. D.; Hoare, S.; Inglese, J.; Iversen, P. W.; Lal-Nag, M.; Li, Z.; Manro, J. R.; McGee, J.; McManus, O.; Pearson, M.; Riss, T.; Saradjian, P.; Sittampalam, G. S.; Tarselli, M.; Trask, O. J.; Weidner, J. R.; Wildey, M. J.; Wilson, K.; Xia, M.; Xu, X., Eds.; Eli Lilly & Company and the National Center for Advancing Translational Sciences: Bethesda (MD), 2004.
(57) Wiegand, I.; Hilpert, K.; Hancock, R. E. W. Agar and Broth Dilution Methods to Determine the Minimal Inhibitory Concentration (MIC) of Antimicrobial Substances. *Nat. Protoc.* **2008**, *3* (2), 163−175.
(58) *Performance Standards for Antimicrobial Susceptibility Testing*, 30th ed.; Clinical and Laboratory Standards Institute: Wayne: PA, 2020.
(59) Wishart, D. S.; Sayeeda, Z.; Budinski, Z.; Guo, A.; Lee, B. L.; Berjanskii, M.; Rout, M.; Peters, H.; Dizon, R.; Mah, R.; Torres-Calzada, C.; Hiebert-Giesbrecht, M.; Varshavi, D.; Varshavi, D.; Oler, E.; Allen, D.; Cao, X.; Gautam, V.; Maras, A.; Poynton, E. F.; Tavangar, P.; Yang, V.; van Santen, J. A.; Ghosh, R.; Sarma, S.; Knutson, E.; Sullivan, V.; Jystad, A. M.; Renslow, R.; Sumner, L. W.; Linington, R. G.; Cort, J. R. NP-MRD: The Natural Products Magnetic Resonance Database. *Nucleic Acids Res.* **2022**, *50* (D1), D665−D677.

https://doi.org/10.1021/acs.jnatprod.6c00531
J. Nat. Prod. 2026, 89, 1995−2007